Proceedings of the 7th International Conference on Mechanics and Materials in Design
Albufeira/Portugal 11-15 June 2017. Editors J.F. Silva Gomes and S.A. Meguid.
Publ. INEGI/FEUP (2017)

PAPER REF: 6488

IDENTIFICATION OF POSSIBLE CAUSES OF FATIGUE FAILURE IN RADIUS ROD PINS FOR TROLLEYBUS REAR AXLES USING PARAMETRIC CALCULATIONS OF FATIGUE LIFE

Miloslav Kepka(*), Miloslav Kepka Jr.

Regional Technological Institute, Research Center of Faculty of Mechanical Engineering (RTI),
University of West Bohemia, Pilsen, Czech Republic
(*)*Email:* kepkam@rti.zcu.cz

ABSTRACT

Fatigue failures were frequently encountered in the pins of radius rods of driving axles of trolleybuses in city of San Francisco. Sufficiently representative stress-time histories for the critical cross section through this part were obtained by measurement carried out during rides with empty as well as fully loaded vehicle. Estimates of relevant fatigue characteristics were developed using information on used material, various surface treatments were taken into consideration. Parametric calculations of fatigue life were therefore feasible with the aid of the available data. The nCode software was used for all calculations. The purpose of these calculations was to ascertain whether these in-service failures in the structural parts of the vehicle could have been predicted (and prevented) during the design stage, and what their main cause had been.

Keywords: fatigue life, fatigue failure, radius rod pin, service load, computational prediction of service fatigue life, nCode software

INTRODUCTION

Radius rods ensure the appropriate geometry of axles with respect to the vehicle underframe. Together with other parts of the axle suspension system (shock absorbers and air spring bellows), they ensure noiseless transmission of force from the axle to the vehicle under any dynamic conditions during the ride (starting, braking, running over irregular surface and others). The radius rod is a weldment consisting of a tube with a head on each end. Metal-rubber bushings are press-fitted into holes in the heads. The configurations of the metal-rubber bushings may vary. The typical one involves overhung conical pins. Vehicles in service suffered fatigue failures of these pins. The fracture location was in the narrow region adjacent to the radius transition to the conical part.

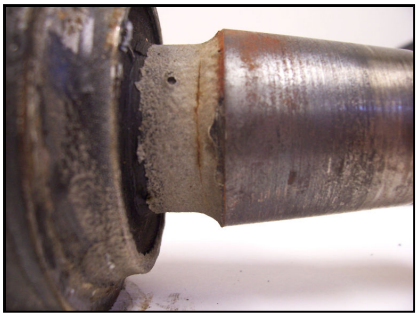

Fig. 1 - Fatigue fracture of a radius rod pin

Figure 1 shows a photograph of a failed pin. After driving 70,000 miles a fatigue damage (initiation of fatigue cracks or complete fatigue fracture) occurred at approximately 50 of the total 612 pieces of installed and operated pins.

Strain gauge testing and fatigue life assessment of heavily stressed structural details and parts of trolleybuses are carried out at various stages throughout the development process (Kepka, 2015). The testing locations include several hundred critical locations on the vehicle, tested either during service load simulations on an electrohydraulic test stand or during prototype vehicle rides on actual routes. In the present case, the measurement was conducted at a later stage because the part in question (the pin of the radius rod of the rear axle) had not been expected to pose any problems based on previous experience. The data gathered in actual service included information about the part's service life to failure. By comparing the information from service and the computational prediction of fatigue life, one could find whether the measurement and fatigue calculations would have been a sufficient basis for identifying the part as a critical one if it had been subject to scrutiny early on.

LOADING CONDITIONS, MEASURED AND ANALYSED DATA

Loading of both radius rods and radius rod pins were measured in real operational conditions. The representative data were obtained during the operation of a trolleybus on a city line of total length of 16.2 miles. The test roads included hilly profile typical for the city of San Francisco, varying quality of the road surface, breaking, starting, cornering etc. The measurements were carried out at two load conditions (payloads): driving with empty and fully loaded vehicle.

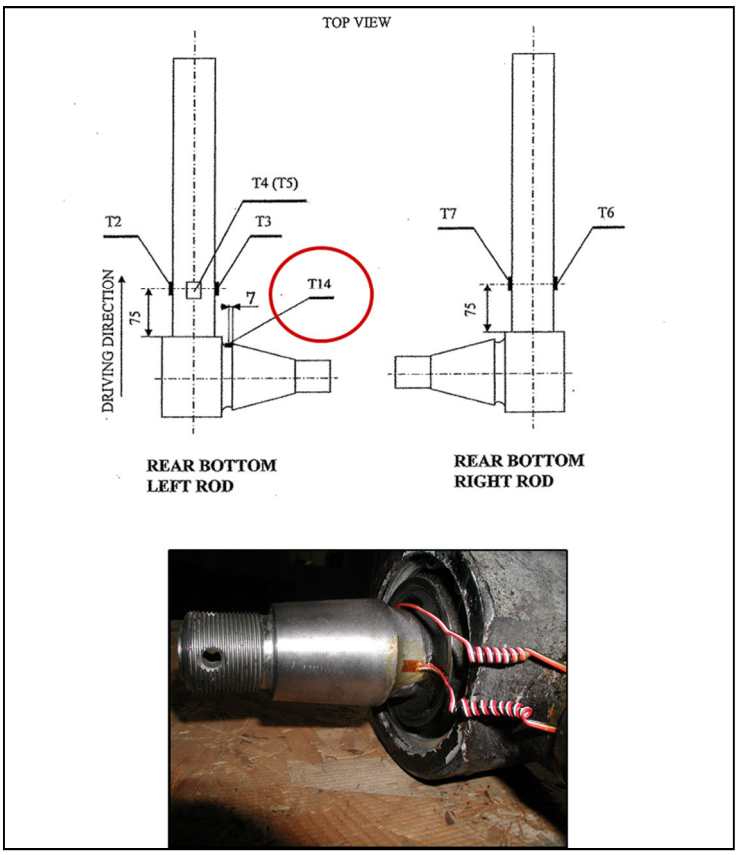

Fig. 2 - Location of strain gauge T14

Figure 2 shows installation of all strain gauges. The strain gauge T14 was installed on the critical structural notch of the pin and therefore local deformations and stresses were measured directly.

Figure 3 shows measured stress-time histories.

Figure 4 shows stress spectra, which were evaluated with nCode software using the rain-flow method. The spectra are necessary for fatigue life calculation.

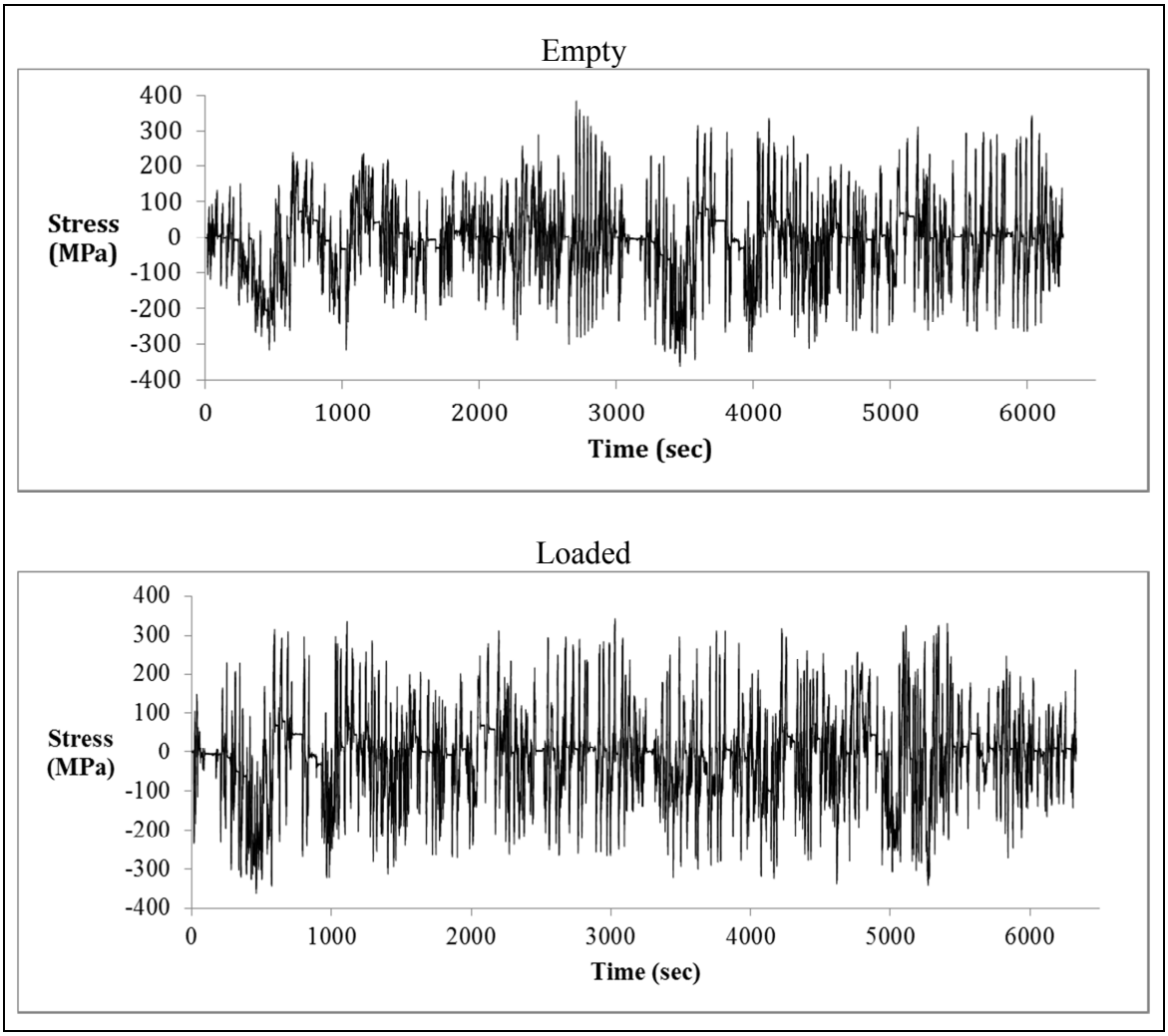

Fig. 3 - Measured stress-time histories - empty vehicle and loaded vehicle - strain gauge T14

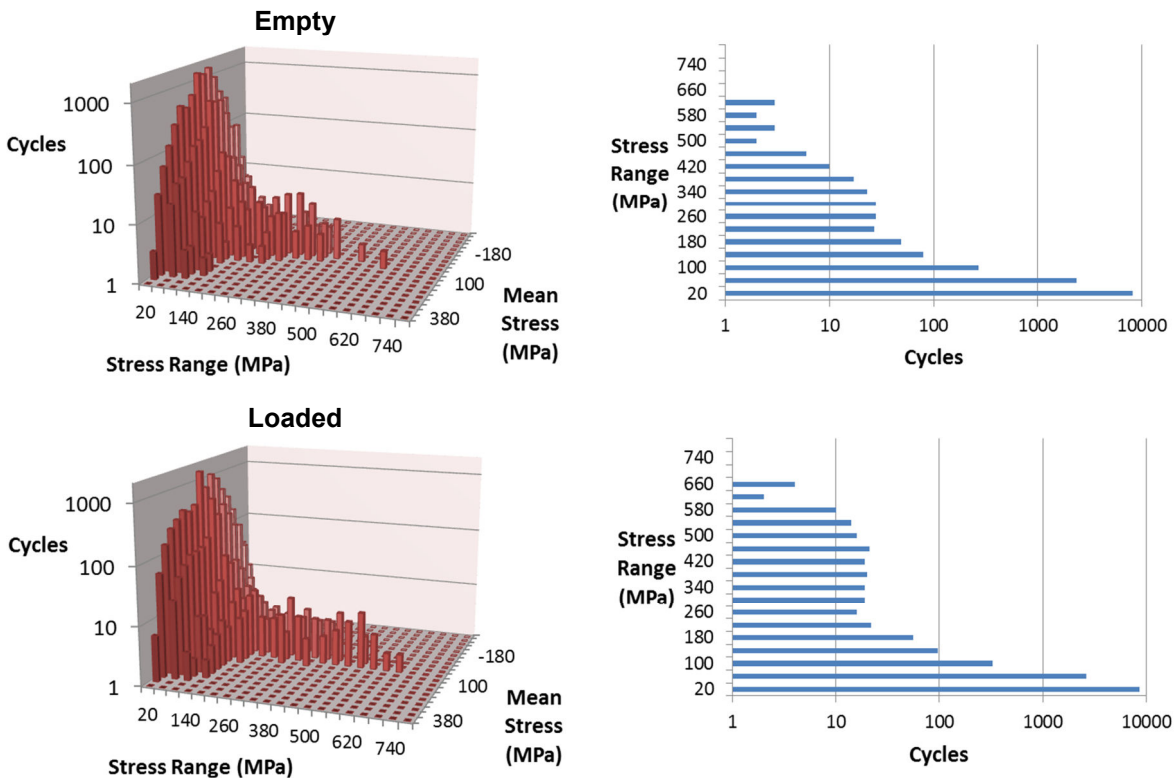

Fig. 4 - Two-parameter and one-parameter stress spectra - empty vehicle and loaded vehicle

FATIGUE LIFE CURVES

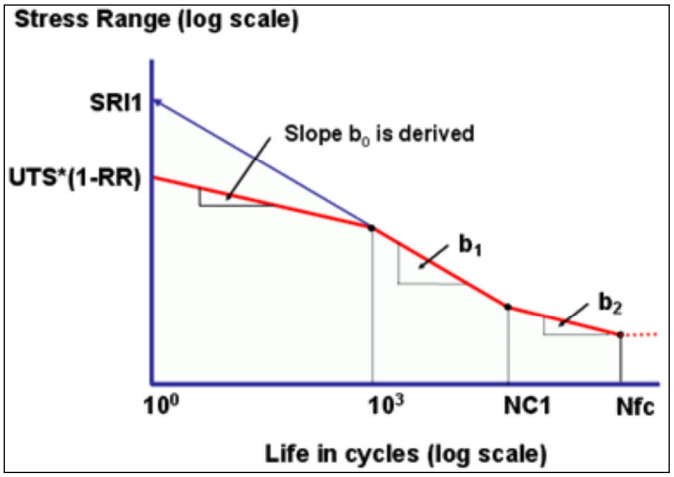

Fig. 5 - Description of fatigue life curve in nCode software

Fig.5 is a copy of description of fatigue life curves used by nCode software. A durability of a material or a component against high cycle fatigue damage is commonly characterized by an σ-N curve, which describes a relationship between stress range $\Delta\sigma$ and cycles to failure N_f. This relationship can be described for $N_f \in (10^3, NC1)$ by the following nCode formula:

$$\Delta\sigma = SRI1 \cdot \left(N_f\right)^{b1}, \tag{1}$$

where SRI1 is an intercept at 1 cycle and $b1$ is a slope.

The pin was made of steel CMo4 according to a Hungarian standard. Ultimate strength of this steel ranges between 700 - 900 MPa. Any relevant information about fatigue behaviour of CMo4 was not found in literature despite of a thorough search and therefore the fatigue curve had to be estimated only.

Material 1

The Uniform Material Law proposed by Bäumel and Seeger in 1990 was used as the first estimation method for determining the fatigue characteristics. The following Table 1 depicts the values, on which UML is based for unalloyed and low-alloy steels.

Table 1 - Uniform Material Law (Bäumel, 1990)

	$\varepsilon_a = \varepsilon_{a,el} + \varepsilon_{a,pl} = \frac{\sigma_f'}{E}(2N)^b + \varepsilon_f'(2N)^c$
σ_f'	$1.5 \cdot R_m$
b	-0.087
ε_f'	$0.59 \cdot \psi$
c	-0.58
σ_D	$0.45 \cdot R_m$
ε_D	$0.45\frac{R_m}{E} + 1.95 \cdot 10^{-4} \cdot \psi$
N_D	$5 \cdot 10^5$
K'	$1.65 \cdot R_m$
n'	0.15
	$\psi = 1$ for: $\frac{R_m}{E} \leq 3 \cdot 10^{-3}$ $\psi = \left(1.375 - 125 \cdot \frac{R_m}{E}\right)$ for: $\frac{R_m}{E} > 3 \cdot 10^{-3}$ and $\psi \geq 0$

Material data generated from UML for a steel with UTS = 800 MPa are shown in Table 2. The material data are in format used by software nCode GlyphWorks for Strain-Life and Stress-Life approach.

Table 2 - Fatigue characteristics of Material 1 (estimation according to UML)

$\varepsilon_a = \varepsilon_{a,el} + \varepsilon_{a,pl} = \frac{\sigma_f'}{E}(2N)^b + \varepsilon_f'(2N)^c$			$\Delta\sigma = SRI1 \cdot \left(N_f\right)^{b1}$		
Fatigue Strength Coefficient	σ_f'	1200 MPa	Stress Range Intercept	$SRI1$	3630 MPa
Fatigue Strength Exponent	b	-0.087	Fatigue Strength Exponent	$b1$	-0.1339
Fatigue Ductility Coefficient	ε_f'	0.5303	Standard Error of Log N_f		0.1
Fatigue Ductility Exponent	c	-0.58			
Cyclic Strength Coefficient	K'	1320 MPa			
Cyclic Strain Hardening Exponent	n'	0.15			

Material 2

The other option to receive a relevant material data was a usage of a German equivalent steel 42CrMo4 with UTS = 1100 MPa. A material σ-N curve was statistically estimated from an experimental data from literature (Boller, 1998) in accordance with standard ISO 12107. Since the value of *UTS* of CMo4 is lower, the statistically evaluated curve was modified by decreasing stress range intercept $SRI1$ while fatigue strength exponent remained the same. The estimated parameters of the fatigue life curve are presented in Table.

Table 3 - Fatigue characteristics of Material 2 (estimation according to experimental data in the literature)

$\Delta\sigma = SRI1 \cdot (N_f)^{b1}$		
Stress Range Intercept	$SRI1$	1584 MPa
Fatigue Strength Exponent	$b1$	-0.063
Standard Error of Log N_f		0.1

The second fatigue strength exponent $b2$ (see Fig.5) was chosen conservatively $b2 = b1$ for both material fatigue curves. There was not any fatigue limit considered in the fatigue damage calculation.

The estimated fatigue life curves are graphically interpreted in Fig.6.

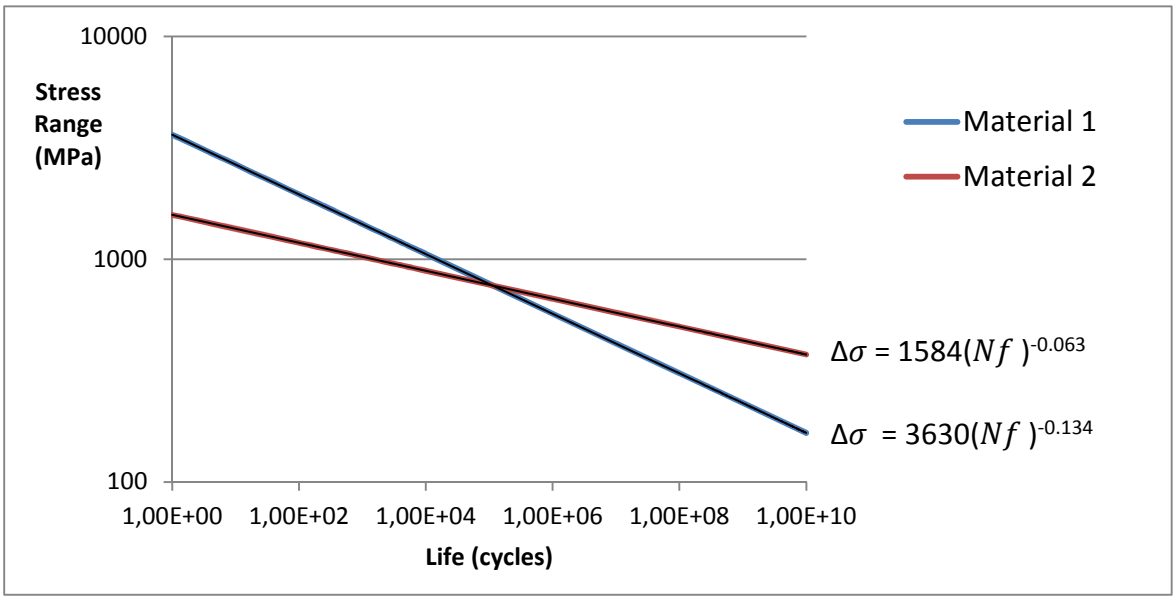

Fig. 6 - Estimated fatigue life curves

FATIGUE LIFE CALCULATIONS

The Palmgren-Miner rule was applied in this case study. According to this hypothesis, it is achieved the fatigue limit state (limit damage, initiation of a macroscopic fatigue crack, final failure) when the following condition is fulfilled:

$$\sum_i \frac{n_i}{N_i} = 1, \tag{2}$$

n_i is number of cycles with stress range $\Delta\sigma_i$ and N_i is number of cycles to failure at the same stress range $\Delta\sigma_i$.

Local stress approach was used for the calculation. The procedure describes schematically Fig.7 (Ruzicka, 2001). The calculation considers local notch stresses and a material σ-N curve.

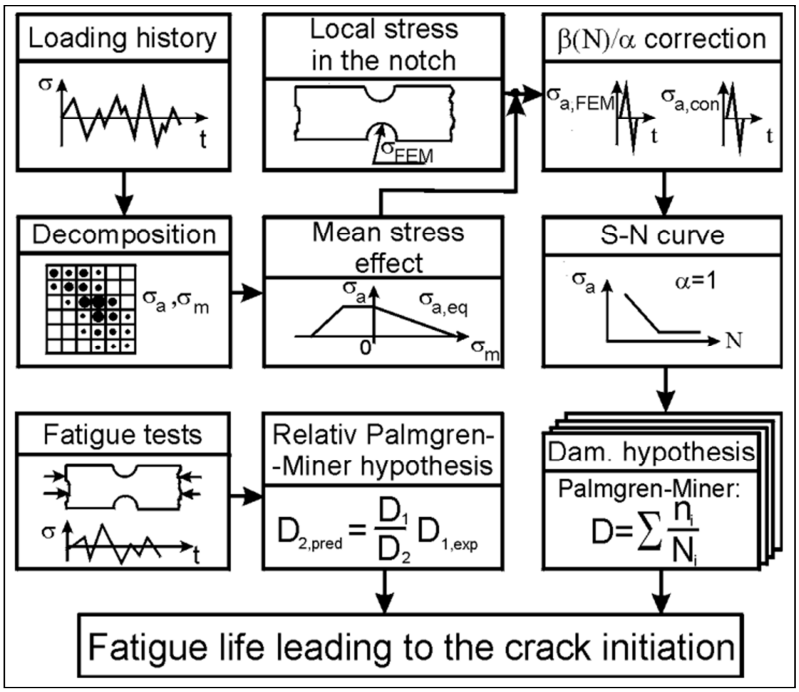

Fig. 7 - General description of local elastic stress approach (Ruzicka, 2001)

The main feature of a cycle that affects fatigue damage is the stress range. However, it is also influenced by the mean stress of each cycle. The Goodman mean stress correction calculates the effective stress amplitude σ_e, which is used in damage calculation (2) instead of the stress amplitude σ_a:

$$\sigma_e = \frac{\sigma_a . UTS}{UTS - \sigma_m}, \tag{3}$$

where *UTS* je ultimate tensile strength of material and σ_m is a mean stress.

All measured local stresses were below the yield strength and therefore no correction of plasticity was required. The nCode software allows taking into consideration a quality of the surface of the assessed materials and components. The fatigue life was estimated twice for both Material 1 and Material 2. In the first calculation there was not any surface correction involved ('polished' surface), in the other the surface finish was set to 'good machined'.

Tables 4 to 7 show estimated fatigue lives for various combinations of service conditions and for defined σ-N curves (two estimated material σ-N curves with two surface finish modifications).

Table 4 - Mean fatigue life for various combinations of service conditions, Material 1, Polished

σ-N curve, Surface	Material 1, Polished					
Empty (%): Loaded (%)	0: 100	20: 80	40: 60	60: 40	80: 20	100: 0
Fatigue Life (1000 miles)	407	384	362	340	318	295

Table 5 - Mean fatigue life for various combinations of service conditions, Material 1, Good Machined

σ-N curve, Surface	Material 1, Good Machined					
Empty (%): Loaded (%)	0: 100	20: 80	40: 60	60: 40	80: 20	100: 0
Fatigue Life (1000 miles)	140	128	117	106	95	83

Table - 6 Mean Fatigue life for various combinations of service conditions, Material 2, Polished

σ-N curve, Surface	Material 2, Polished					
Empty (%): Loaded (%)	0: 100	20: 80	40: 60	60: 40	80: 20	100: 0
Fatigue Life (1000 miles)	460	757	1054	1351	1647	1944

Table 7 - Mean fatigue life for various combinations of service conditions, Material 2, Good Machined

σ-N curve, Surface	Material 2, Good Machined					
Empty (%): Loaded (%)	0: 100	20: 80	40: 60	60: 40	80: 20	100: 0
Fatigue Life (1000 miles)	152	176	202	226	251	275

The stress spectra for empty and loaded vehicle have different shapes (Fig.4). The slopes of fatigue life curves of materials 1 and 2 are different and the fatigue curves intersect (Fig.6). If the fatigue curve of Material 1 used for predicting service life, than the operation with an empty vehicle comes computationally as more damaging. When the fatigue curve of Material 2 is used, the operation with a loaded vehicle is more damaging for the critical cross section of the investigated component.

The required service life of mechanical parts of trolleybuses was 500 000 miles driven. This value was reached only for Material 2, polished surface conditions. Furthermore, the predictions of service life in the tables are mean values of fatigue life, a value with only a 50% probability of survival. It was therefore decided to implement further calculations in this case study.

SCALE FACTOR CALCULATION

The scale factor calculation can provide a usable feedback to a designer. It determines the value by which the stress-time history has to be multiplied to achieve specified target life, in this case 500 000 miles. Mean σ-N curves were used in the fatigue life estimation in the previous chapter. However, to reach a suitable reliability it is necessary to work with design σ-N curves, as we want to make a life prediction based on a particular percentage probability of survival. The deviation from the mean (50%) life is determined in terms of the value of standard errors. According to a respected standard (FKM-Guideline, 2012) a sufficient certainty of survival is equal to 97.5 % which corresponds to -2 standard errors. Therefore

$$\log N_{97.5} = \log N_{50} - 2 \cdot (\text{Standard Error of Log } Nf). \tag{4}$$

The design fatigue life curves for Material 1 and Material 2 are shown in Fig. 8.

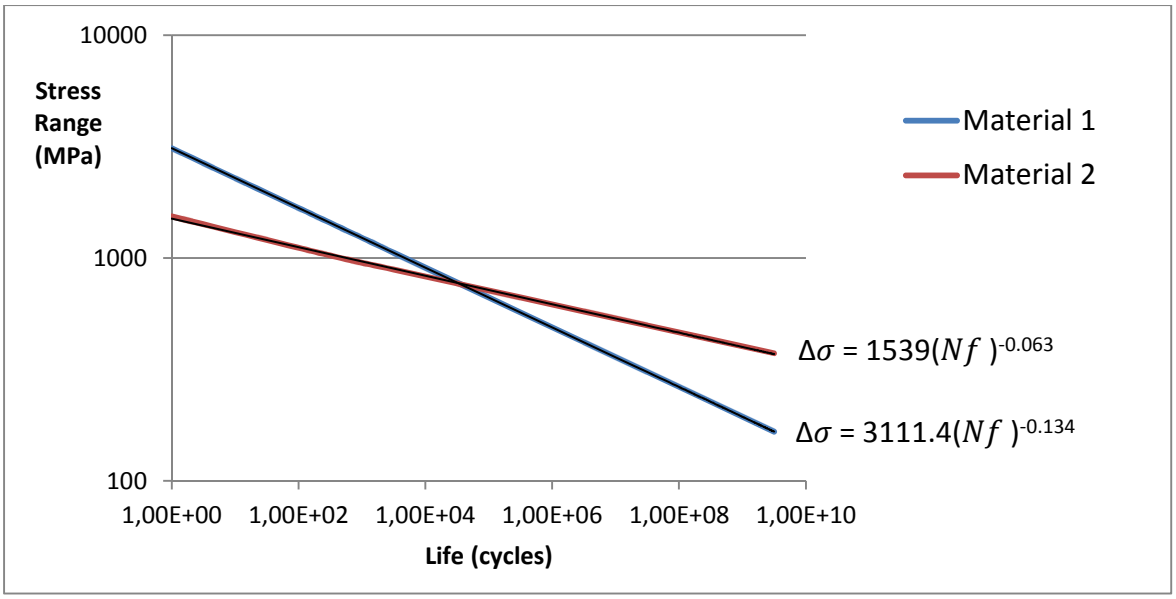

Fig. 8 - Design σ-N curves of Material 1 and Material 2

The scale factor was calulated in the nCode software for both design fatigue live curves and for more realistic 'good machine' surface conditions. The Table 8 summarises the settings applied for the calculations and the results.

Table 8 - Scale Factor Calculation Conditions and Results

Settings		
Material Data	Material 1	Material 2
Surface Finish	Good Machined	Good Machined
Mean Stress Correction	Goodman	Goodman
Standard Error of Log *N*	0.1	0.25
Service Conditions	Loaded	Empty
Target Life	500 000 miles	500 000 miles
Results		
Scale Factor	0.70	0.83

The reduction of local notch stress of about 30% (Table 8, Material 1) is needed to meet the durability target, therefore significant changes in the component geometry are required. It can be achived by decresing nominal stress or changes in geometry (structural notch) of the component.

RESULTS

Several partial and step-by-step related results were presented in this case study. The local stress spectra were evaluated for the critical cross section of the considered component. The representative stress-time histories were measured in real traffic conditions. The fatigue characteristics of the material used for production of the component were estimated. Service life predictions of the investigated component were made for different operating load conditions of the vehicle.

Based on the inverse calculations of fatigue damage was so-called scale factor determined as the recommended value of reduction of local stresses, in order to ensure the required service life with a defined reliability.

CONCLUSION

It can be concluded that the causes of operational failures of the assessed radius rod pins were high stress concentrations in the critical (notched) cross section and a poor surface quality of the component.

The presented case study showed how the nCode software can be used for parametric calculations of fatigue life and how the design of cyclically loaded components can be supported.

ACKNOWLEDGMENTS

The present contribution has been prepared under project LO1502 “Development of the Regional Technological Institute” under the auspices of the National Sustainability Program me I of the Ministry of Education of the Czech Republic aimed to support research, experimental development and innovation.

REFERENCES

[1]-Kepka, M., Spirk, S.: Tests and computer simulations of electric buses. Proceedings M2D2015 - 6th International Conference on Mechanics and Materials in Design, Porta Delgada/Azores/Portugal, 26-30 July 2015

[2]-Bäumel, A., Seeger, T.: Materials data for cyclic loading. Supplement 1. Amsterdam; New York: Elsevier, 1990. ISBN: 0444886036

[3]-Boller, Chr.: Der Einfluß von Probengröße und Oberflächenrauhigkeit auf Lebensdauerabschätzungen bei Betrachtung der örtlichen Beanspruchungen. Heft 46. Darmstadt: Veröffentlichungen des Instituts für Stahlbau und Werkstoffmechanik der Technischen Hochsule Darmstadt, 1998. 292 s.

[4]-Růžička, M. - Papuga, J., New Concept of a Local Elastic Stress Approach for Fatigue Life Calculation. In: Abstract Collection of the ICAF 2001 Conference. ICAF 2001 Conference. Toulose, 25.06.2001 - 29.06.2001. Toulouse: The French Association for Aeronautics and Astronautics. 2001, s. 56-58.

[5]-FKM-Guideline: Analytical Strength Assessment of Components in Mechanical Engineering. 6th. ed. 2012, ISBN 978-3-8163-0649-8